JACS
JOURNAL OF THE AMERICAN CHEMICAL SOCIETY
pubs.acs.org/JACS
Article

Non-Equilibrium Growth Processes to Glyceraldehyde and Glycerol as Building Blocks of Interstellar Sugars and Phospholipids

Xilin Bai, Qi'ang Gong, Jinghui Lu, Jiuzhong Yang, Yang Pan, Zhenrong Sun, Ralf I. Kaiser,* and Tao Yang*

Cite This: J. Am. Chem. Soc. 2026, 148, 22979−22989
Read Online
ACCESS | Metrics & More | Article Recommendations | Supporting Information

ABSTRACT: Complex organic molecules (COMs) such as aldoses and polyols are essential prebiotic compounds and serve as fundamental molecular building blocks for key biomolecules, including sugars and lipids. Despite their detection in star-forming regions and carbonaceous meteorites, the mechanisms of formation of these COMs in extraterrestrial environments remain largely controversial. Here, we demonstrate the bottom-up synthesis of a diverse set of COMs in the formaldehyde−water (H_2CO-H_2O) ice analogs subjected to simulated galactic cosmic rays (GCRs), including aldoses and polyols (glycolaldehyde, ethylene glycol, glyceraldehyde, and glycerol), as well as other compounds like glyoxal, methoxymethanol, (methoxymethoxy)methanol, formic acid, and methanetriol. The identification of these oxygen-bearing COMs was achieved using synchrotron vacuum ultraviolet photoionization reflectron time-of-flight mass spectrometry (SVUV-PI-ReToF-MS) during the temperature-programmed desorption (TPD) phase. Their unambiguous assignment was further confirmed by isotopic labeling experiments and by fitting the photoionization efficiency (PIE) curves of the parent product and fragment ions. The efficient synthesis of these COMs reveals constraints of the molecular complexity and reaction pathways available for forming aldoses and polyols in space, expanding our understanding of how such biorelevant precursors form in the extraterrestrial environments and their potential role in the abiotic origin of life on Earth.

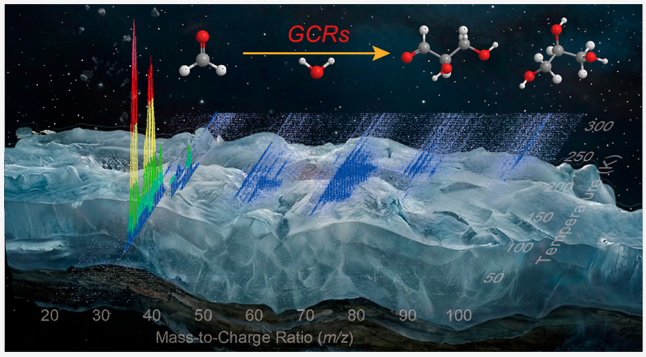

INTRODUCTION

The ubiquitous presence of complex organic molecules (COMs) in the extraterrestrial environments has greatly challenged the fundamental role of gas-phase reaction mechanisms, since their predicted fractional abundances are a few orders of magnitude lower than the observed ones toward the star-forming regions like TMC-1 and Sgr B2(N).[1−3] Regarded as key precursors to molecular building blocks relevant to the origin of life, a large majority of COMs is believed to form in the interstellar dust grain ice mantles via radiative (electrons, protons, photons) or thermal processes of interstellar ices, which were eventually delivered to Earth by asteroids and comets.[4,5] Such an abiotic formation scenario greatly motivates the understanding of replicating the observed abundances of COMs and their astronomical detection. However, the elucidation of their formation pathways as well as their impact in the astrochemical reaction networks is still elusive.[6]

Two-carbon complex organic molecules (C2 COMs) of sugars and polyols—glycolaldehyde ($HOCH_2CHO$) and ethylene glycol ($HOCH_2CH_2OH$)—have been detected in various environments including cold molecular clouds,[7] solar-mass protostars,[8] and Kuiper Belt Objects like 67P/Churyumov-Gerasimenko.[9] Their formation mechanisms have been suggested by sequential carbon atom addition pathways involving carbon monoxide (CO) and atomic hydrogen (H),[10−12] radical recombination pathways following the carbon monoxide to methanol (CH_3OH) conversion via the formyl radical ($H\dot{C}O$) and the hydroxymethyl radical ($\cdot CH_2OH$),[13−18] and radical recombination pathways initiated by irradiation of CH_3OH-rich ices.[19−23] The radical-driven pathways are thought to be more efficient than the non-energetic one toward the formation of larger members of three-carbon complex organic molecules (C3 COMs), such as glyceraldehyde ($HOCH_2CH(OH)CHO$) and glycerol ($HOCH_2CH(OH)CH_2OH$). They represent fundamental precursors to sugars and lipids, involving not only in the construction of nucleic acids and cell membranes but also in key biological processes such as energy metabolism as well

Received: March 1, 2026
Revised: April 19, 2026
Accepted: April 27, 2026
Published: May 13, 2026

https://doi.org/10.1021/jacs.6c04482
J. Am. Chem. Soc. 2026, 148, 22979−22989

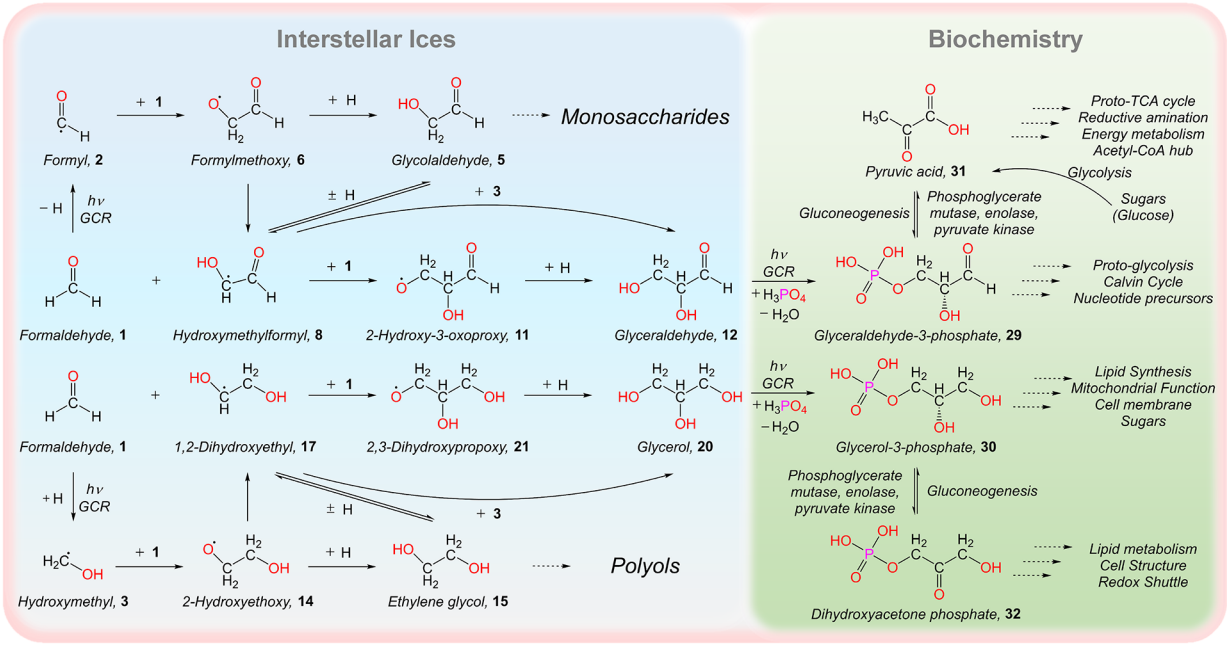

Figure 1. Formation of glyceraldehyde and glycerol in interstellar ices and their relevance to central carbon metabolism. Energetic processing of interstellar ice analogs containing simple C1 precursors, such as formaldehyde (**1**), by ultraviolet irradiation or galactic cosmic rays (GCRs) generates reactive radical intermediates, including formyl (**2**) and hydroxymethyl (**3**). Subsequent radical−radical/radical−molecule reactions and stepwise hydrogenation driven carbon−carbon bond formation, yielding C2 and C3 oxygenated products such as glycolaldehyde (**5**), ethylene glycol (**15**), glyceraldehyde (**12**), and glycerol (**20**). These reactions establish low-temperature, nonequilibrium pathways linking monosaccharides and polyols in extraterrestrial environments. In biochemistry, glyceraldehyde and glycerol occupy a central position through their phosphorylated derivatives—glyceraldehyde-3-phosphate (**29**), glycerol-3-phosphate (**30**), and dihydroxyacetone phosphate (**32**)—which participate in glycolysis, gluconeogenesis, lipid biosynthesis, and associated energy-conversion processes.

(Figure 1).[24,25] Although glyceraldehyde and glycerol have not yet been detected in the interstellar medium (ISM), their presence in carbonaceous chondrites like Murchison suggests a potential interstellar origin following the transfer to the early Earth by meteorites and comets.[26−28]

Early simulation experiments identified C3 COMs in processed astrophysical model ices using offline techniques like high-performance liquid chromatography (HPLC) or gas chromatography−mass spectrometry (GC−MS), attributing their formation as contamination or secondary reactions upon exposure to the atmosphere.[29−31] Recent studies introduced CH_3OH into water (H_2O) or H_2O and ammonia (NH_3) ice mixtures, revealing the detection of glyceraldehyde and glycerol.[24,32,33] However, their room-temperature analysis of organic residues prohibits a detailed understanding of the reaction mechanisms. Employing Fourier transform infrared (FTIR) spectroscopy and quadrupole mass spectrometry (QMS) during the temperature-programmed desorption (TPD) phase, Fedoseev et al. extended the radical recombination pathways following the CO to CH_3OH hydrogenation route and demonstrated the formation of glycerol and plausible glyceraldehyde by the reaction of H and CO with glycolaldehyde.[25,34] Kaiser et al., Maity et al., Sullivan et al., and Chen et al. reported the potential synthesis of glycerol but no glyceraldehyde in the electron-processed pure CH_3OH or CH_3OH−CO ices exploiting the QMS, FTIR spectroscopy, two-dimensional gas chromatography coupled to time-of-flight mass spectrometry, and/or vacuum ultraviolet single-photon ionization coupled with reflectron time-of-flight (PI-ReToF-MS) mass spectrometry.[20,25,35] However, definitive identification proved challenging due to the high degree of structural similarity between C2 and C3 COMs, which resulted in overlapping IR spectral features and complicated TPD spectra regardless of the ionization method (electron impact ionization or photoionization). Especially, the structural isomer identification of glyceraldehyde and glycerol in the gas phase still remains elusive, thus introducing substantial uncertainties in their formation throughout low-temperature ices in cold molecular clouds and astronomical detection in star-forming regions.

Here, we report the efficient bottom-up synthesis of C2 COMs (glycolaldehyde ($HOCH_2CHO$), ethylene glycol ($HOCH_2CH_2OH$), glyoxal (HCOCHO), and methoxymethanol (CH_3OCH_2OH)) and C3 COMs (glyceraldehyde ($HOCH_2CH(OH)CHO$), glycerol ($HOCH_2CH(OH)CH_2OH$), and (methoxymethoxy)methanol ($CH_3OCH_2OCH_2OH$)), as well as formic acid (HCOOH) and methanetriol ($CH(OH)_3$) in H_2CO−H_2O ice analogs exposed to proxies of galactic cosmic rays (GCRs).[36] Using synchrotron vacuum ultraviolet photoionization reflectron time-of-flight mass spectrometry (SVUV-PI-ReToF-MS),[37−41] we identified structural isomers of subliming products by isotopic labeling experiment and photoionization efficiency (PIE) curve fitting and warrant the definitive detection of glyceraldehyde and glycerol by their dissociative photoionization fragments. Our results suggest that C2 and C3 COMs can form via radical−radical or radical-molecule pathways, facilitated by water acting as both an energy-transfer medium and a stabilizing matrix, except for the formation of HCOOH and $CH(OH)_3$. The isomer-selective identification of these products is crucial for understanding how more complex biorelevant molecules form in extraterrestrial ices. These molecules may not only remain trapped in the ice and become incorporated into comets and meteorites—potentially

https://doi.org/10.1021/jacs.6c04482
J. Am. Chem. Soc. 2026, 148, 22979−22989

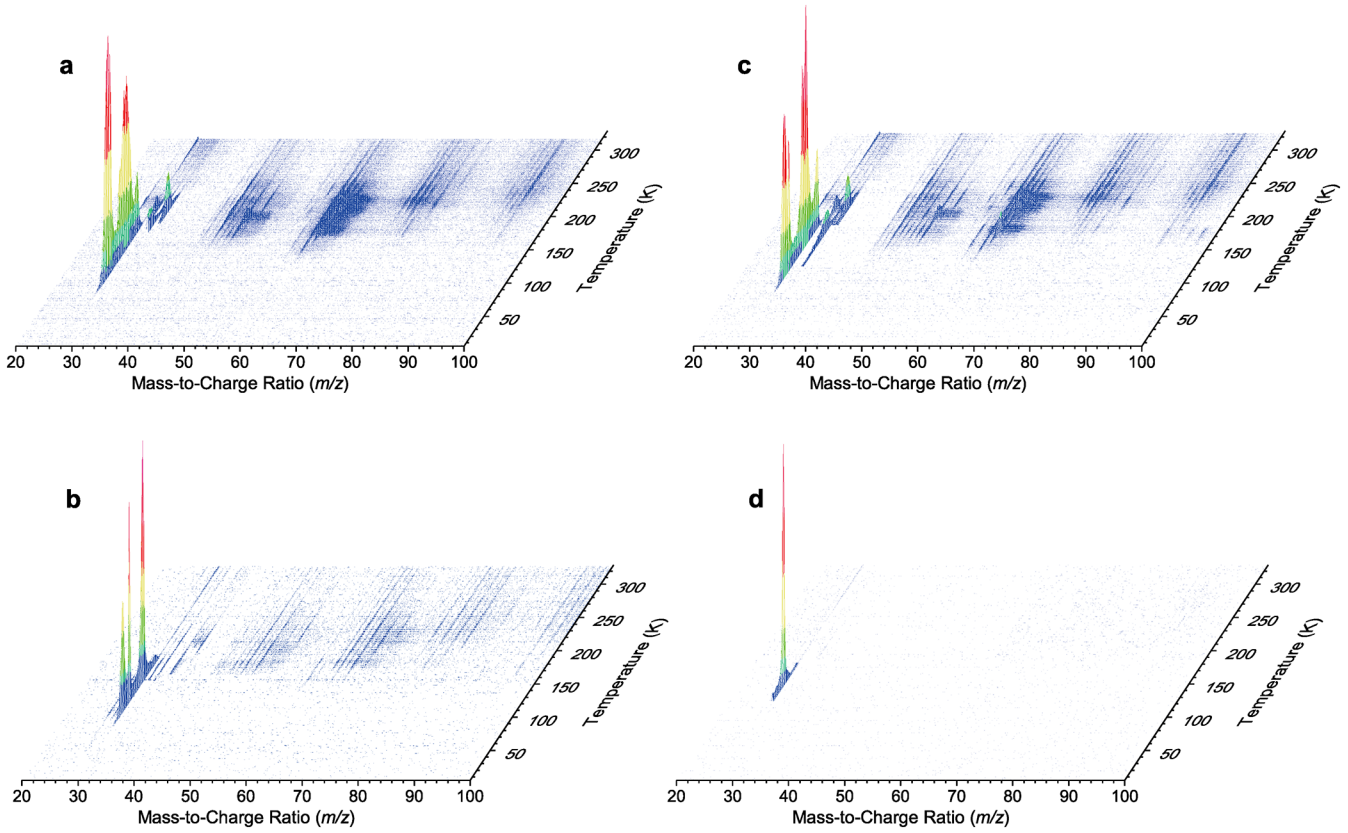

Figure 2. Synchrotron vacuum ultraviolet photoionization reflectron time-of-flight mass spectrometry (SVUV-PI-ReToF-MS) data during the temperature-programmed desorption (TPD) phase. Data were recorded for the irradiated (a) formaldehyde−water (H_2CO-H_2O), (b) D_2CO-D_2O, (c) $H_2CO-H_2{}^{18}O$, and (d) the unirradiated (blank) H_2CO-H_2O ices at the photoionization energy of 11.50 eV.

contributing to the origin of life on early Earth—but may also sublime into the gas phase in star-forming regions such as Orion KL thereby influencing the chemical evolution of star-forming regions.

RESULTS

SVUV-PI-ReToF-MS

We exploited the photon energy of 11.50 eV to probe newly formed molecules desorbed from the H_2CO-H_2O, D_2CO-D_2O, and $H_2CO-H_2{}^{18}O$ ice analogs exposed to electron radiation, whose product ions were mass-analyzed via the reflectron time-of-flight mass spectrometry (ReToF-MS) to gain considerable signal resolution (Figure 2). At the photon energy of 11.50 eV, we identified pronounced ion counts at the mass-to-charge ratio (m/z) = 30 (CH_2O^+), 31 (CH_3O^+), 32 (O_2^+/CH_4O^+), 33 (HO_2^+/CH_5O^+), 44 ($CO_2^+/C_2H_4O^+$), 46 ($CH_2O_2^+/C_2H_6O^+$), 47 ($CH_3O_2^+/C_2H_7O^+$), 58 ($C_2H_2O_2^+/C_3H_6O^+$), 60 ($C_2H_4O_2^+/C_3H_8O^+$), 61 ($CHO_3^+/C_2H_5O_2^+/C_3H_9O^+$), 62 ($CH_2O_3^+/C_2H_6O_2^+$), 72 ($C_2O_3^+/C_3H_4O_2^+/C_4H_8O^+$), 73 ($C_2HO_3^+/C_3H_5O_2^+/C_4H_9O^+$), 74 ($C_2H_2O_3^+/C_3H_6O_2^+/C_4H_{10}O^+$), 75 ($C_2H_3O_3^+/C_3H_7O_2^+$), 89 ($C_2HO_4^+/C_3H_5O_3^+/C_4H_9O_2^+/C_6HO^+$), 90 ($C_2H_2O_4^+/C_3H_6O_3^+/C_4H_{10}O_2^+/C_6H_2O^+$), and 91 ($C_2H_3O_4^+/C_3H_7O_3^+/C_6H_3O^+$) (Figure 3), in contrast to solely the formaldehyde cation (H_2CO^+, m/z = 30) in the unirradiated (blank) experiment (Figure 2).

First of all, the ionization energies of oxygen (O_2) and carbon dioxide (CO_2) were, respectively, measured to be 12.0697 ± 0.0002 eV and 13.777 ± 0.001 eV.[42−44] Since these energies are higher than the available photon energy of 11.50 eV, neither O_2 nor CO_2 can be ionized and detected in our experiments. Second, isotopic labeling experiments provided further constraints on the molecular compositions of observed product and fragment ions. For species desorbed from the irradiated D_2CO-D_2O ices, we observed molecular ions at m/z = 32, 34, 36, 38, 48, 50, 60, 64, 66, 68, 76, 78, 80, 82, 94, 96, and 98. Considering that only the hydrogen/deuterium exchange between H_2CO-H_2O and D_2CO-D_2O ices, we can exclude the detection of ions at m/z = 46 ($C_2H_6O^+$), 47 ($C_2H_7O^+$), 61 ($CHO_3^+/C_3H_9O^+$), 72 ($C_2O_3^+$), 73 ($C_2HO_3^+$), 74 ($C_4H_{10}O^+$), 89 ($C_2HO_4^+/C_6HO^+$), and 90 ($C_2H_2O_4^+/C_4H_{10}O_2^+/C_6H_2O^+$), since their deuterated counterparts were not observed in the D_2CO-D_2O ices (Figure S1, Table S1). Third, an examination of the fitted TPD spectra provided additional constraints on the molecular formulas of observed ions. The similar bimodal TPD spectra between 200 and 300 K at m/z = 72, 73, and 74 indicate that they should follow the sequential dissociative fragmentation pattern (Figure 3). However, since we have ruled out the existence of ion signals at m/z = 72 ($C_2O_3^+$), 73 ($C_2HO_3^+$), and 74 ($C_4H_{10}O^+$) based on isotopic labeling experiments, their dissociative ion signals at m/z = 72 ($C_4H_8O^+$), 73 ($C_4H_9O^+$), and 74 ($C_2H_2O_3^+$) should not exist either. Similarly, ion signals at m/z = 89 ($C_4H_9O_2^+$) and 91 ($C_2H_3O_4^+/C_6H_3O^+$) can also be precluded since ion signals at m/z = 90 can only be ascribed to $C_3H_6O_3^+$ based on our analysis. Lastly, most of the TPD spectra do not shift with respect to m/z when comparing molecular ions in the irradiated H_2CO-H_2O and $H_2CO-H_2{}^{18}O$ systems (Figures 3 and S2), implying that H_2O likely facilitates

https://doi.org/10.1021/jacs.6c04482
J. Am. Chem. Soc. 2026, 148, 22979−22989

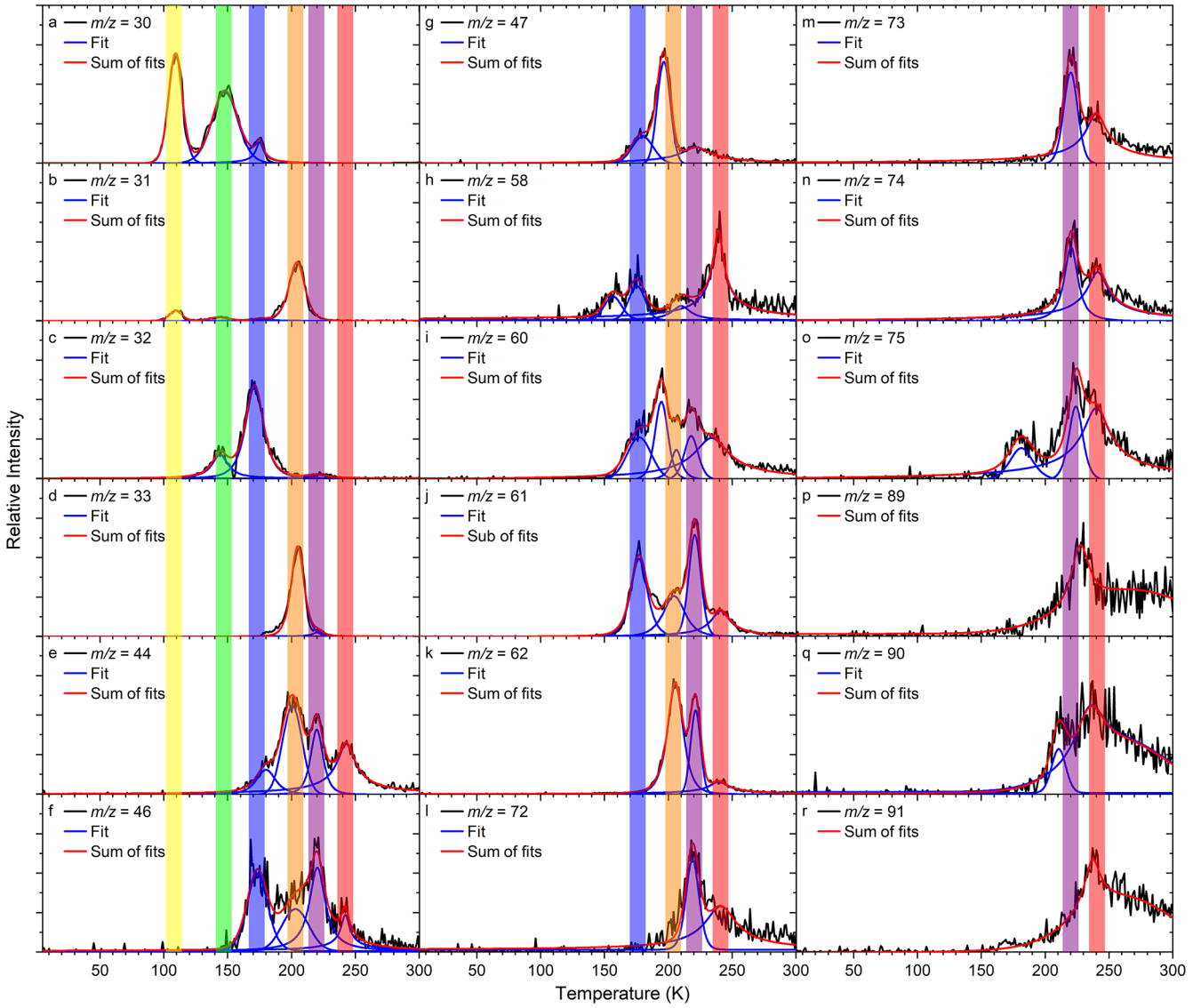

Figure 3. TPD spectra at distinct mass-to-charge ratio (m/z) observed in processed H_2CO-H_2O ices at the photoionization energy of 11.50 eV. Blue lines represent data fitted with multiple Pearson peaks, and red lines indicate the total fit of deconvoluted profiles. Colored bars categorize molecular species that cosublime at specific temperatures, based on their dominant origin: fragmentation of a common parent molecule, volcanic effect associated with water ice, or cosublimation with water. The color sequence represents increasing sublimation temperatures: yellow (~109 K), green (~147 K), blue (~171 K), orange (~205 K), purple (~221 K), and red (~241 K).

formation as a catalytic medium or reaction cage by suppressing recombination pathways.[17] The overlapped TPD spectra after scaling in both ices imply the detection of ion signals $CH_2O^{18}O^+$ (m/z = 48), $CH_3O^{18}O^+$ (m/z = 49), and $CH_3{}^{18}O_2{}^+$ (m/z = 51) in the $H_2CO-H_2{}^{18}O$ system (Figure S3). Therefore, based on the analysis of SVUV-PI-ReToF-MS we can conclude that ion signals at m/z = 30 (CH_2O^+), 31 (CH_3O^+), 32 (CH_4O^+), 33 (CH_5O^+/HO_2^+), 44 ($C_2H_4O^+$), 46 ($CH_2O_2^+$), 47 ($CH_3O_2^+$), 58 ($C_2H_2O_2^+/C_3H_6O^+$), 60 ($C_2H_4O_2^+/C_3H_8O^+$), 61 ($C_2H_5O_2^+$), 62 ($CH_2O_3^+/C_2H_6O_2^+$), 72 ($C_3H_4O_2^+$), 73 ($C_3H_5O_2^+$), 74 ($C_3H_6O_2^+$), 75 ($C_2H_3O_3^+/C_3H_7O_2^+$), 89 ($C_3H_5O_3^+$), 90 ($C_3H_6O_3^+$), and 91 ($C_3H_7O_3^+$) were detected in the irradiated H_2CO-H_2O modeled ices.

Structural Isomer Identification of One-Carbon (C1) and Two-Carbon Complex Organic Molecules

Our SVUV-PI-ReToF-MS at the photon energy of 11.50 eV along with isotopic labeling experiments defined the molecular formulas of parent product and fragment ions in the irradiated H_2CO-H_2O ices (Table S1). PIE curves can quantify the ion count intensity as a function of the photon energy at distinct m/z.[37,40,41] Since we can only obtain the PIE curve at a specific m/z during the TPD phase, both the SVUV photon energy range and desorption temperature range must be chosen carefully in order to minimize signal interference. Therefore, we distinguish the temperature intervals in the color bars to facilitate a more precise analysis of subliming species (Figures 3, S1, and S2).

The TPD spectra highlighted in yellow (~109 K), green (~147 K), and blue (~171 K) bars at m/z = 30 can be attributed to the naturally subliming H_2CO, H_2CO produced from the volcanic effect in water ice, and H_2CO cosublimed

https://doi.org/10.1021/jacs.6c04482
J. Am. Chem. Soc. 2026, 148, 22979−22989

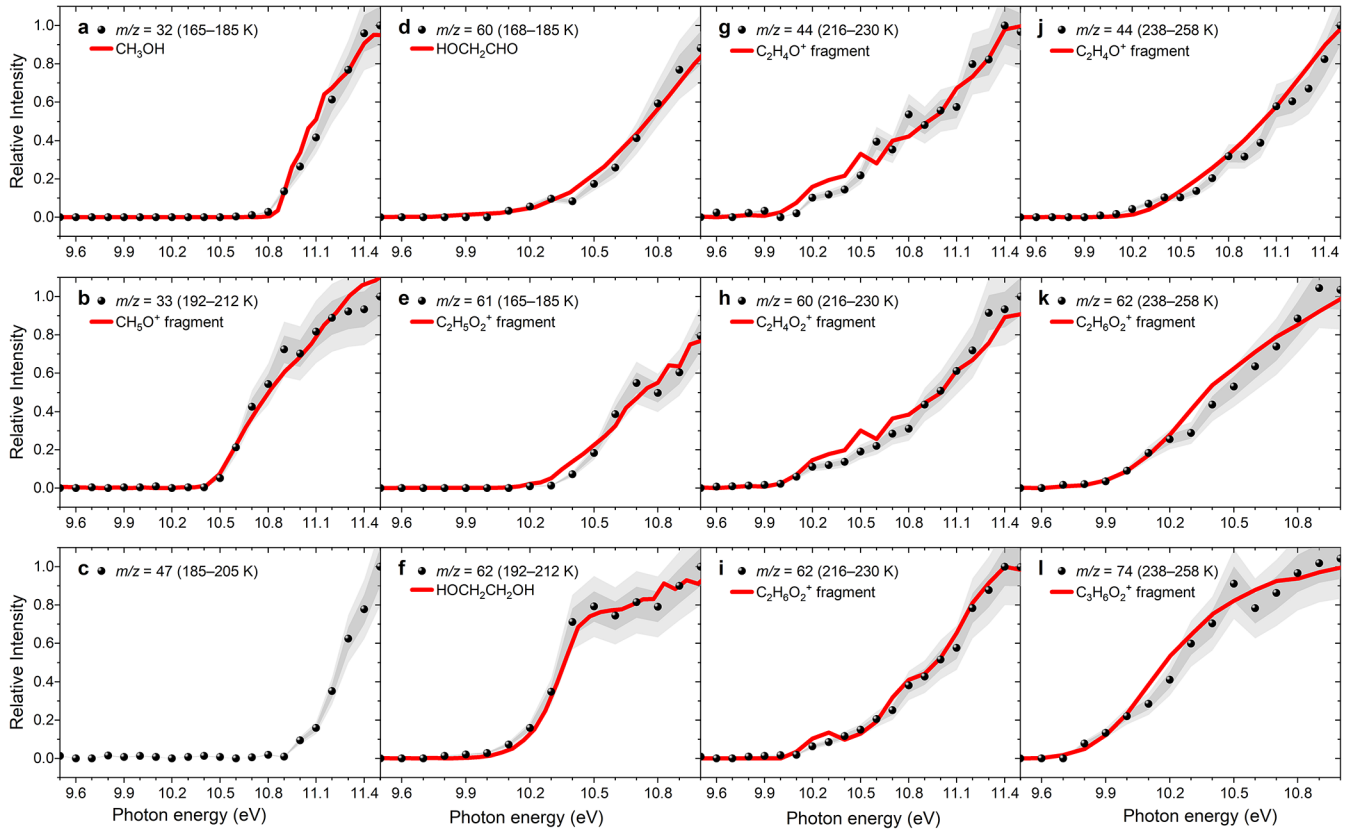

Figure 4. Photoionization efficiency (PIE) curves correspond to parent ions of C1 species or fragment ions of C2 species at m/z of (a) 32, (b) 33, and (c) 47; parent or fragment ions of C2 species at m/z of (d) 60, (e) 61, and (f) 62; fragment ions of glyceraldehyde at m/z of (g) 44 ($C_2H_4O^+$), (h) 60 ($C_2H_4O_2^+$), and (i) 62 ($C_2H_6O_2^+$); and fragment ions of glycerol at m/z of (j) 44 ($C_2H_4O^+$), (k) 62 ($C_2H_6O_2^+$), and (l) 74 ($C_3H_6O_2^+$). Solid cycles represent experimental data, and red lines show fits to reference PIE curves. The dark-gray and light-gray shaded regions indicate the 1σ and 2σ standard deviations of the PIE curve (averaged across individual scans), respectively. Additional PIE curves are provided in the Supporting Information.

with water, respectively.[45] Ion signals at m/z = 31 can be assigned as ^{13}C-isotopic contributions from the H_2CO reactant, while the TPD peak highlighted in the orange bar (CH_3O^+, m/z = 31) is likely associated with a dissociative fragment of ethylene glycol.[46] The TPD peak at m/z = 32 highlighted in both green and blue bars correspond to the CH_4O product(s), which indicates the formation of methanol as revealed by our PIE scan (Figure 4a). The single TPD peak at m/z = 33 highlighted in the orange bar (~205 K) can be associated with dissociative fragments CH_5O^+ from ethylene glycol rather than the HO_2 radical, which depicts an ionization energy of 11.352 ± 0.007 eV.[43] We further confirm CH_5O^+ as the dissociative fragment of ethylene glycol by the PIE scan at m/z = 33, which bears an ionization energy of 10.50 eV and matches well with the gas phase study of ethylene glycol in the flash pyrolysis setup.[46] TPD signals highlighted in the blue bars at m/z = 46 can be connected to $CH_2O_2^+$, most likely HCOOH. This can be well warranted by the PIE curve at m/z = 46 (Figure S4), which also excluded its isomers of low adiabatic ionization energies (AIEs), i.e. the Criegee intermediate formaldehyde oxide (·CH_2OO·, 9.98 eV) and dioxirane (c-CH_2O_2, 10.82 eV).[47,48] It is noteworthy that the pronounced TPD spectrum of m/z = 47 ($CH_3O_2^+$) peaking at 197 K coincides with the dissociative fragmentation of methanetriol $CH(OH)_3$ leading to $CH(OH)_2^+$ plus ·OH (Figure S3).[38] Not only the fragment TPD spectra of H_2CO–H_2O and D_2CO–D_2O ices overlap nicely with those in the CH_3OH–O_2 and CD_3OD–O_2 ices, but the appearance energy of 11.00 ± 0.10 eV derived from our PIE at m/z = 47 correlates well with the predicted value of 11.03 ± 0.04 eV for $CH(OH)_2^+$ in the study of the irradiated CH_3OH–O_2 ice (Figure 4c).[38]

For C2 COMs, the only structural isomer carrying the cation form of $C_2H_2O_2^+$ (m/z = 58) is glyoxal (HCOCHO), as confirmed by comparing our experimental TPD spectrum with the reference one (Figure S5). This assignment is validated by the matching desorption peaks for both acetylenediol (HOCCOH) and HCOCHO reported by Wang et al. in electron-irradiated CO–H_2O ice.[49] Ion signals highlighted in the blue bar at m/z = 60 may attribute to cations of glycolaldehyde ($HOCH_2CHO$; 10.20 eV), ethene-1,2-diol (HOCHCHOH; 9.62 eV), acetic acid (CH_3COOH; 10.65 eV), and methyl formate ($HCOOCH_3$; 10.84 eV) with AIEs provided in parentheses (Figure S6 and Table S2). After matching the experimental onset and PIE curve with the reference PIE curve of glycolaldehyde,[50] we can claim that glycolaldehyde contributes significantly to the ion signals at m/z = 60. For ion signals at m/z = 61 highlighted in the blue bar, the experimental onset of 10.30 ± 0.05 eV and PIE curve can match well with those of the $C_2H_5O_2^+$ fragment (appearance energy of 10.24 ± 0.05 eV), which follows prompt dissociative ionization of methoxymethanol (CH_3OCH_2OH) via a tunneling mediated H loss.[51] As of ion signals at m/z = 62 highlighted in the orange bar, we may attribute ions signals at

https://doi.org/10.1021/jacs.6c04482
J. Am. Chem. Soc. 2026, 148, 22979–22989

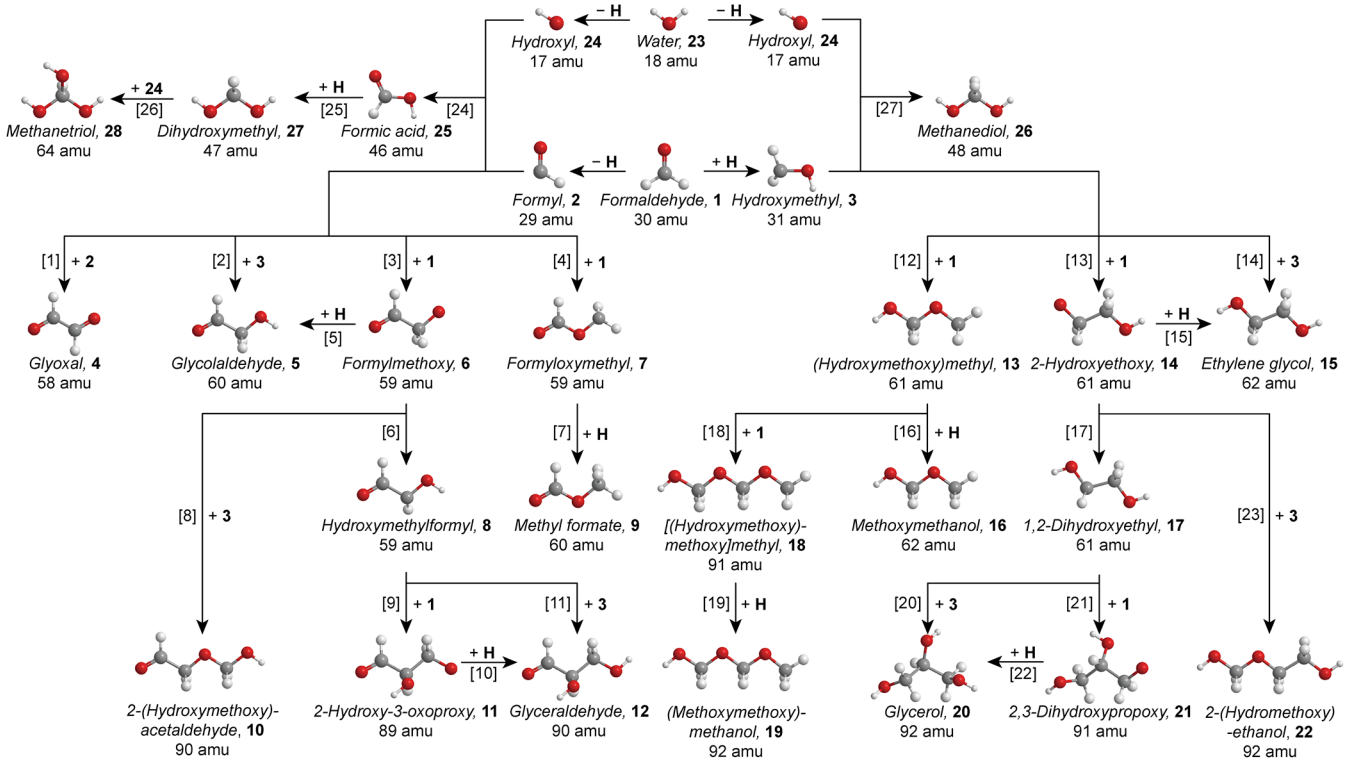

Figure 5. Derived formation pathways from C1 precursors to C2 and C3 oxygenated products in irradiated H_2CO–H_2O ices. Top panel: Primary radiolysis of H_2CO–H_2O ices produces radicals and products including formyl (**2**), hydroxymethyl (**3**), hydroxyl (**24**), formic acid (**25**), and methanetriol (**28**). Middle panel: Subsequent radical–radical and radical–molecule reactions generate C2 species including glyoxal (**4**), glycolaldehyde (**5**), ethylene glycol (**15**), and methoxymethanol (**16**). Bottom panel: Further radical–radical and radical–molecule reactions extend the network to C3 species, including glyceraldehyde (**12**), (methoxymethoxy)methanol (**19**), and glycerol (**20**). This progression from simple radicals to COMs illustrates the stepwise accumulation of chemical complexity within interstellar H_2CO–H_2O ice analogs.

m/z = 62 to ethylene glycol ($HOCH_2CH_2OH$, 9.85 eV), dimethyl peroxide (CH_3OOCH_3, 9.31 eV), ethyl hydroperoxide (C_2H_5OOH, 9.70 eV), or 1,1-ethanediol ($CH_3CH(OH)_2$, 10.65 eV) (Figure S7, Tables S3 and S4). Nevertheless, the comparison of the experimental onset and PIE curves with reference ones can only lead to the detection of ethylene glycol.[46] In addition, its fragmentation TPD spectra highlighted in the orange bars at m/z = 61, 44, 33, and 31 are well correlated with the gas-phase dissociative fragmentation pattern of ethylene glycol, whose PIE curves at m/z = 62, 44, 33, and 31 match well with each other (Figures 4 and S8).[46]

Structural Isomer Identification of Three–Carbon COMs

We noticed that SVUV-PI-ReToF-MS of subliming products of the H_2CO–H_2O ices at 11.50 eV present a series of TPD spectra peaking at 221 (purple bar) and 241 K (red bar), implying significant dissociative photoionization from parent cations of common COMs. Further extraction and Pearson VII fitting of these TPD spectra give rise to pronounced fragment ions of $C_2H_4O^+$ (m/z = 44), $C_2H_6O^+$ (m/z = 46), $C_2H_4O_2^+$ (m/z = 60), $C_2H_5O_2^+$ (m/z = 61), $C_2H_6O_2^+$ (m/z = 62), $C_3H_4O_2^+$ (m/z = 72), $C_3H_5O_2^+$ (m/z = 73), and $C_3H_4O_2^+$ (m/z = 74) peaking at both temperatures. Isotopic labeling experiments (D_2CO–D_2O, H_2CO–$H_2{}^{18}O$) demonstrate unambiguously the expected TPD spectra with corresponding isotopic shifts (Figures S1 and S2). These dissociative fragmentation profiles at 241 K (red bar) correlate well with those of glycerol formed in the methanol model ices peaking at about 237 K.[25] The parent glycerol cation is so low in intensity compared to its fragment ions that the direct detection of glycerol is elusive.[25] In addition, we performed PIE scanning at m/z = 44, 62, and 74 near 241 K, yielding PIE curves of these fragment ions that agree nicely with those obtained in the gas phase photoionization of pure glycerol carried out in the effusive molecular beam apparatus.[52] Enlightened by the gas phase studies and fragmentation pattern of glycerol, we conducted single-photon ionization of pure glyceraldehyde in the TPD phase and PIE scans of the dissociative fragments in the gas phase (Figures S9 and S10). Once again, the unique coincidence of mass spectrometry of fragment ion signals at m/z = 33, 44, 60, 61, 62, and 72, as well as their PIE curves at m/z = 44, 60, and 62 between the subliming product at 221 K and the pure glyceraldehyde sample, has been well established. Therefore, we present compelling evidence of the formation and gas phase detection of glyceraldehyde and glycerol. Extending this analytical protocol to ion signals at m/z = 91 (red bar) reveals the ionization onset of 10.10 eV and PIE curve matching the $C_3H_7O_3^+$ fragment of (methoxymethoxy)-methanol, further confirming its formation as found in the irradiated H_2CO ice (Figure S11).

DISCUSSION

Formaldehyde is not only regarded as a key intermediate molecule along the CO to CH_3OH hydrogenation route, but detected as abundant species in high- and low-mass protostars.[2] Accreting CO molecules form a layer of CO ice on the icy grain surfaces while simultaneously undergo hydrogenation to produce HĊO and $\cdot CH_2OH$ radicals in a nonenergetic manner.[34] These two radicals can also form upon irradiation of CH_3OH-rich ices by energetic particles, and it

https://doi.org/10.1021/jacs.6c04482
J. Am. Chem. Soc. 2026, 148, 22979–22989

shall not be omitted that the hydrogenation of H_2CO may also lead to the possible formation of the methoxy radical ($CH_3O\cdot$). However, H-addition to H_2CO could proceed preferentially through $\cdot CH_2OH$ rather than $CH_3O\cdot$, which could isomerize to $\cdot CH_2OH$ through intramolecular hydrogen atom transfer.[53,54] The elusive detection of methyl formate and dimethyl peroxide warrants the lack of $CH_3O\cdot$ in the CO hydrogenation route unless it is generated by the CH_3OH decomposition,[23,55,56] while small molecules like H_2O or HCOOH can facilitate the isomerization of $CH_3O\cdot$ to $\cdot CH_2OH$ via formation of a doubly hydrogen-bonded transition state.[23,55,57,58] Therefore, the CO hydrogenation could initially proceed to $H\dot{C}O$, $\cdot CH_2OH$ and CH_3OH in atomic−addition reactions which play an important role in dark cloud chemistry.

The formation mechanism of COMs with repeating C−C and C−O backbones is critical for understanding the synthesis competition among key biomolecules. The radical−radical reaction of $H\dot{C}O$ and $\cdot CH_2OH$ can easily lead to the formation of glyoxal, glycolaldehyde, and ethylene glycol via reactions [1], [2], and [14], respectively (Figures 5 and S12). The alternative reaction mechanism involves the addition of $H\dot{C}O$ or $\cdot CH_2OH$ to H_2CO forming C−C bonding and C−O bonding radicals as $HCOCH_2O\cdot$, $HOCH_2CH_2O\cdot$, $\cdot CH_2OCHO$ and $\cdot CH_2OCH_2OH$ via reactions [3], [13], [4], and [12], which respectively yields glycolaldehyde, ethylene glycol, methyl formate, and methoxymethanol upon hydrogenation (reactions [5], [15], [7], and [16]) (Figures 5 and S13). Interestingly, C−O bonding radicals are theoretically suggested to be formed with lower entrance barriers but less thermally stable than C−C bonding radicals.[17] As we found substantial glycolaldehyde, ethylene glycol, and methoxymethanol, both C−C and C−O bond formation processes should be considered in our irradiated H_2CO−H_2O ices. In this regard, the elusive detection of methyl formate can attribute to relatively low yield of $H\dot{C}O$ radicals, which can be exhausted by its dimerization leading to glyoxal.[16] In fact, the integrated TPD signal for glycolaldehyde is about 15% of that for ethylene glycol, not to mention that glycolaldehyde possesses a more delocalized highest occupied molecular orbital and tends to have a larger photoionization cross section under the same ionization energy when comparing with ethylene glycol.[59] Nevertheless, our recent studies revealed the formation of H_2CO oligomers ($H-(CH_2O)_n-H$; n = 2−4) within irradiated pure H_2CO ice analogs, in which we suggested a radical-induced H_2CO polymerization mechanism leading to methoxymethanol through C−O bonding.[41] Therefore, the formation of C2 COMs can proceed via radical−radical or radical-molecule reactions, followed by hydrogenation.

We now discuss potential reaction mechanisms from simple organic molecules to the formation of C3 COMs. Butscher et al. realized tentative identification of glyceraldehyde from the VUV photolysis of H_2CO in Ar matrix, proposing the pathway as the glycolaldehyde reaction with $H\dot{C}O$ followed by another $H\dot{C}O$ addition and CO elimination.[16] They later presented the possible formation of glyceraldehyde and glycerol from VUV photolysis of H_2CO in Ar and Xe matrices, claiming formation routes as radical recombination of $HO\dot{C}HCH_2OH$ with $H\dot{C}O$ or $\cdot CH_2OH$ respectively, where the $HO\dot{C}HCH_2OH$ intermediate radical is formed through H atom addition to glycolaldehyde or H atom abstraction from ethylene glycol.[17] Layssac et al. conducted the VUV photolysis experiments on the H_2CO−H_2O mixture ices, and put forward a radiation temperature-dependent mechanism involving radical−formaldehyde reactions as common initiation step for aldose and polyol formation rather than radical recombination reactions only.[18] For the formation of glycerol, Kaiser et al. and Zhu et al. proposed a bottom-up sequential reaction initiated by $\cdot CH_2OH$ to ethylene glycol, which loses H upon irradiation to form $HO\dot{C}HCH_2OH$ followed by recombination with another $\cdot CH_2OH$ leading eventually to glycerol.[25,35] In our experiments, we propose that $H\dot{C}O$ or $\cdot CH_2OH$ adds with H_2CO through C−C bonding to form $HCOCH_2O\cdot$ and $HOCH_2CH_2O\cdot$ via reactions [3] and [13], which can also respectively isomerize to $HCO\dot{C}HOH$ and $HOCH_2\dot{C}HOH$ via reactions [6] and [17]. Since the $H\dot{C}O$ radical is relatively low-abundance in our ices, the radical−radical reaction mechanism can possibly lead to $HCOCH_2OCH_2OH$ (90 amu), $HOCH_2CH_2OCH_2OH$ (92 amu), glyceraldehyde, and glycerol (reactions [8], [23], [11], and [20]). However, the former two cannot be preferentially formed since they involve C−O bonding formation which exhibit relatively higher entrance barriers. The alternative pathway can be proposed as the addition of H_2CO to $HCO\dot{C}HOH$ or $HOCH_2\dot{C}HOH$ through C−C bonding forming $HCOCHOHCH_2O\cdot$ and $HOCH_2CHOHCH_2O\cdot$, leading eventually to glyceraldehyde (reactions [9] and [10]) and glycerol (reactions [21] and [22]), respectively (Figures 1 and 5). In contrast, (methoxymethoxy)methanol formation proceeds through a distinct C−O-based pathway: H_2CO adds to $\cdot CH_2OH$ via a C−O bond to generate the $\cdot CH_2OCH_2OH$ intermediate (reaction [12]), which subsequently undergoes a second C−O addition with another H_2CO molecule (reaction [18]) prior to hydrogenation, completing chain propagation and termination. Therefore, our studies unveil two compelling pathways leading to C3 COMs, the formation of glyceraldehyde and glycerol through the C−C backbone and the formation of (methoxymethoxy)methanol through chain propagation and termination via the C−O backbone. Here, H_2O likely facilitates the formation of COMs as a catalytic medium or reaction cage by suppressing recombination pathways.

Strikingly found, $H\dot{C}O$ may react with $\cdot OH$ to form HCOOH[60,61] via reaction [24] as verified in the H_2CO−H_2O, D_2CO−D_2O, and H_2CO−$H_2{}^{18}O$ ices. However, we did not observe any $CH_2(OH)_2$ ion signals near 181 K as confirmed in the CH_3OH−O_2 ices,[62] which should be facilely formed via radical recombination of $\cdot CH_2OH$ with $\cdot OH$ via reaction [27]. One possible explanation is the HCOOH hydrogenation leading to the energetically favorable radical $H\dot{C}(OH)_2$ that is stabilized by the hydrogen bonding with the neighboring H_2O in the H_2O ice environment (reaction [25]), or $H\dot{C}(OH)_2$ is generated as one of the HCOOH dimer dissociation products.[63,64] The definitive formation of $CH(OH)_3$ but detection via its dissociative fragment can be verified in the H_2CO−$H_2{}^{18}O$ ices where ion signals at m/z = 49 ($CH_3{}^{16}O{}^{18}O^+$) and 51($CH_3{}^{18}O_2{}^+$) were both detected, corresponding to $^{18}\cdot OH$ and $^{16}\cdot OH$ dissociative channels, respectively. The elusive detection of $CH_2(OH)_2$ formed via radical recombination of $\cdot CH_2OH$ and $\cdot OH$ strongly indicates competing mechanisms between $\cdot CH_2OH$ + $\cdot OH$, $\cdot CH_2OH$ + H, and $\cdot CH_2OH$ + $\cdot CH_2OH$. Hydrogen atoms could greatly consume $\cdot CH_2OH$ to generate CH_3OH out of question, but self-recombination of $\cdot CH_2OH$ should not be dominant over $\cdot CH_2OH$ + $\cdot OH$ due to excessive H_2O matrix. In the CH_3OH−O_2 ices, $CH_2(OH)_2$ was found to be formed via $O(^1D)$ insertion into CH_3OH barrierlessly, and its TPD signals appear

https://doi.org/10.1021/jacs.6c04482
J. Am. Chem. Soc. 2026, 148, 22979−22989

to be rather weak at 10.86 eV even if the ionization energy of its most stable conformer is 10.66−10.74 eV.[62]

The experiments conducted in this study demonstrate that COMs, particularly sugars, polyols, and other compounds related to life can be efficiently synthesized in H_2CO−H_2O mixed ices through ionization irradiation. The relative abundance of H_2CO molecules in the ice mantles of both high- and low-mass protostars varies between 2 and 7% compared to water,[65] establishing H_2CO as a pivotal precursor in interstellar ices. These ice mantles are subjected to processing by high-energy GCRs and hydrogenation reactions,[34] resulting in the fragmentation of H_2CO molecules and the generation of reactive radicals such as HĊO and ·CH_2OH. These radicals are instrumental in the formation of several COMs reported here, likely occurring within the ice mantles of star-forming regions. Consequently, it is anticipated that glyceraldehyde, glycerol, and even (methoxymethoxy)-methanol are prevalent within the ISM. Once synthesized on the surface of icy dust grains, a fraction of these molecules may sublimate into the gas phase during the transition of molecular clouds to star-forming regions, making them detectable via rotational spectroscopy. In our experimental study, C2 COMs (glyoxal, glycolaldehyde, ethylene glycol, and methoxymethanol) and C3 COMs (glyceraldehyde, glycerol, and (methoxymethoxy)methanol) were synthesized and identified in the processed H_2CO−H_2O ice analogs. Consequently, it is reasonable to hypothesize that if the temperature of hot cores is sufficient to induce sublimation, these organic molecules will coexist in the gas phase. Notably, glycolaldehyde and ethylene glycol have already been successfully detected toward Sgr B2, suggesting that glyceraldehyde and glycerol are also likely to be present in similar interstellar environments and could be detected by the Atacama Large Millimeter/submillimeter Array (ALMA).

The glyceraldehyde formed in our electron-irradiated H_2CO−H_2O ices is produced under achiral experimental conditions. Consequently, this product is expected to be racemic, as is typical for formose-type chain reactions.[33,66] However, in actual interstellar environments, circularly polarized ultraviolet light (UV-CPL) may impart a chiral bias. Astronomical observations have detected significant circular polarization in star-forming regions such as Orion OMC-1 and NGC 6334-V, with polarized regions extending much larger than the size of the protosolar nebula.[67] Laboratory studies have shown that UV irradiation of interstellar ice analogs produces racemic amino acids, and that the use of UV-CPL instead of unpolarized light can induce small enantiomeric excesses (ee's) in these amino acids.[68] Neutral amino acids isolated in solid parahydrogen can exhibit remarkably high anisotropy factors (up to 0.1) under conditions relevant to space.[69] For sugars, meteoritic analyses reveal substantial D-enantiomer excesses in aldonic acids that increase with carbon number, pointing to an asymmetric photochemical origin,[27,70] and recent asymmetric photolysis of racemic isovaline films with CPL produced opposite ee values of up to 2%.[71] Future experiments using UV-CPL on similar H_2CO−H_2O ice mixtures could therefore help elucidate whether enantioselective pathways exist for glyceraldehyde and its higher homologues.

CONCLUSIONS

In conclusion, we unambiguously identify key C2 and C3 COMs formed in the electron-irradiated H_2CO−H_2O ices using synchrotron vacuum ultraviolet photoionization reflectron time-of-flight mass spectrometry (SVUV-PI-ReToF-MS), including glycolaldehyde, ethylene glycol, glyoxal, methoxymethanol, glyceraldehyde, glycerol, and (methoxymethoxy)-methanol as well as formic acid and methanetriol. Distinct dissociative photoionization pathways resolve the long-standing isomeric ambiguity between glyceraldehyde and glycerol, establishing their definitive gas-phase detection during the TPD phase. These results establish that radical−radical and radical-molecule reaction pathways—primarily involving · CH_2OH and HĊO intermediates generated via H_2CO radiolysis—efficiently construct biorelevant carbon skeletons. The H_2CO−H_2O system functions as both reactant reservoir and reaction medium, where water facilitates energy transfer and hydrogen donation, while formaldehyde provides the carbon backbone for sequential chain elongation. This bottom-up formation mechanism operates ubiquitously in hydrogen-rich, oxygen-bearing ices prevalent throughout cold molecular clouds. Sublimation of processed ice mantles in star-forming regions—triggered by protostellar heating or shocks—releases these COMs into the gas phase, rendering them detectable via high-resolution interferometry (ALMA). Given the widespread occurrence of interstellar H_2CO−H_2O ices, glyceraldehyde and glycerol likely constitute unidentified components of the interstellar organic inventory. Delivery of these molecules to early Earth via comets and meteorites would have provided fundamental building blocks for prebiotic chemistry, bridging the gap between processed interstellar ices and the molecular origin of life.

MATERIALS AND METHODS

Experiments (Table S5) were conducted at the Shanghai-Hawaii-Hefei Advanced Research Center for Astrochemistry (SHHARC),[37−39] employing the VUV beamline BL03U at the National Synchrotron Radiation Laboratory.[72] In summary, the SHHARC consists of a stainless ultrahigh vacuum chamber, maintained at pressures of a few 10^{-11} Torr, and is equipped with contamination-free turbomolecular pumps (Osaka Vacuum, TG1300M, TG420M) backed by a dry scroll pump (Leybold, Ecodry 40 Plus). Within the chamber, a polished silver substrate is affixed to an oxygen-free high thermal conductivity copper coldfinger, enabling both vertical and horizontal movement. This movement is facilitated by an ultrahigh-vacuum compatible bellows (McAllister, BLT106) and a double differentially pumped rotary platform (Thermionics Vacuum Products, RNN-600/FA/MCO), respectively. The coldfinger is interfaced with a two-stage closed-cycle helium refrigerator (Sumitomo Heavy Industries, RDK-415E), allowing the system to achieve temperatures as low as 4.7 ± 0.1 K. Temperature monitoring is conducted using a cryogenic temperature sensor (Lakeshore, DT-470).

During the deposition, the silver target was initially cooled to 4.7 K before the deposition. Monomeric formaldehyde in the gas phase was prepared from paraformaldehyde (Aladdin, 95%) using a water-bath heater maintained at 70 °C under vacuum conditions, achieving a preparation purity exceeding 99%.[18] Formaldehyde and water (Macklin, HPLC) were introduced and condensed onto the silver substrate via two separate leak valves and glass capillary arrays (10 mm array diameter) at pressures of (1.0 ± 0.1) × 10^{-8} Torr and (4.0 ± 0.2) × 10^{-8} Torr respectively, achieving an actual depositing ratio of ([H_2CO]/[H_2O]) of 1.0:5.8 ± 0.9 (Supporting Information Methods). This ratio was determined by a calibrated electron-impact quadrupole mass spectrometer (Pfeiffer, QMG 220 M2) (Figure S14). Prior to experiments using $H_2{}^{18}O$ (Aladdin, 97.0 atom % ^{18}O), the lines and vacuum chamber were purged with $H_2{}^{18}O$ vapor to allow any ^{16}O/^{18}O isotopic exchange to occur before the preparation of H_2CO−$H_2{}^{18}O$ ice mixture. The experiment with D_2CO−D_2O ice was

https://doi.org/10.1021/jacs.6c04482
J. Am. Chem. Soc. 2026, 148, 22979−22989

also processed according to this procedure. The thickness of the ice mixture was monitored in situ by laser interferometry using a He−Ne laser (632.8 nm). By employing the refractive indexes of n_{H_2CO} = 1.33 ± 0.04 and n_{H_2O} = 1.27 ± 0.02,[73] the ice thickness was determined to be 743 ± 50 nm (Supporting Information Methods). Subsequent to deposition, the ice mixtures were positioned for electron irradiation at an inclination of 70° relative to the normal of the ice surface. This was achieved using 5 keV electrons (SPECS GmbH, eq 22/35 electron source) at a current of 100 nA for 30 min. The ice thickness significantly exceeds the average electron penetration depth of 324 ± 32 nm, as determined via Monte Carlo simulation performed in CASINO 2.42 (Table S6).[74] After irradiation, the coldfinger was annealed to 320 K at a rate of 1 K min^{-1}. Sublimating molecules were monitored using SVUV-PI-ReToF-MS. The blank experiment, i.e., the nonirradiation experiment, followed the same procedure.

The sublimating species ionized by SVUV were mass analyzed using a ReToF mass spectrometer (Jordan TOF Products, Inc.), operating with 2.5 μs extraction pulses generated by a pulse delay generator (Quantum Composers, 9528) at a repetition rate of 15 kHz. The resulting signal was amplified and discriminated using an F-100T amplifier-discriminator (Advanced Research Instruments Corporation), and subsequently recorded using a multichannel personal computer scalar (FAST ComTec, P7889). During the thermal desorption process, the SVUV photon energy was initially set to 11.50 eV to establish the volatilization temperature range of the species under investigation. Subsequently, within the temperature interval relevant to the species of interest, the SVUV energy was incrementally adjusted across the defined range in 0.10 eV steps with the photon energy- and temperature-dependent mass spectra being recorded concurrently. The TPD spectra, derived from scanning the SVUV energy, were normalized to the TPD spectra at 11.50 eV and the photon flux, leading to derivation of the PIE curves for all detected molecules. The TPD spectra were deconvoluted using the Pearson VII function, a flexible peak-shape model that allows for continuous interpolation between Gaussian and Lorentzian profiles via an adjustable shape parameter.[75] This approach enables an accurate representation of peak broadening and asymmetry observed in the experimental data. The fitting was performed using a nonlinear least-squares curve-fitting procedure, which minimizes the sum of the squares of deviation of the curve from the data ordinates, and the resulting parameters were used to determine peak positions and relative intensities.

■ ASSOCIATED CONTENT

Supporting Information

The Supporting Information is available free of charge at https://pubs.acs.org/doi/10.1021/jacs.6c04482.

Deposition ratio calibration of mixed ices, ice thickness determination, TPD spectra (Figures S1, S2, and S9), ion signals during TPD (Figures S3, S5, and S14), PIE curves (Figures S4, S8, S10, and S11), adiabatic ionization energies of $C_2H_4O_2$ isomers (Figure S6 and Table S2), adiabatic ionization energies of $C_2H_6O_2$ isomers (Figure S7 and Table S3), reaction schemes (Figures S12 and S13), molecular formula and corresponding mass-to-charge ratios of products (Table S1), energies, geometries, and frequencies of 1,1-ethanediol ($CH_3CH(OH)_2$) (Table S4), list of experiments (Table S5), and average dose per molecule (Table S6) (PDF)

■ AUTHOR INFORMATION

Corresponding Authors

Ralf I. Kaiser − *Department of Chemistry, University of Hawaii at Manoa, Honolulu, Hawaii 96822, United States;* orcid.org/0000-0002-7233-7206; Email: ralfk@hawaii.edu

Tao Yang − *State Key Laboratory of Precision Spectroscopy, East China Normal University, Shanghai 200062, China; Collaborative Innovation Center of Extreme Optics, Shanxi University, Taiyuan, Shanxi 030006, China; State Key Laboratory of Radio Astronomy and Technology, Xinjiang Astronomical Observatory, Chinese Academy of Sciences, Urumqi, Xinjiang 830011, China;* orcid.org/0000-0003-4101-2385; Email: tyang@lps.ecnu.edu.cn

Authors

Xilin Bai − *State Key Laboratory of Precision Spectroscopy, East China Normal University, Shanghai 200062, China*

Qi'ang Gong − *State Key Laboratory of Precision Spectroscopy, East China Normal University, Shanghai 200062, China*

Jinghui Lu − *National Synchrotron Radiation Laboratory, University of Science and Technology of China, Hefei, Anhui 230029, China*

Jiuzhong Yang − *National Synchrotron Radiation Laboratory, University of Science and Technology of China, Hefei, Anhui 230029, China;* orcid.org/0000-0002-7076-3412

Yang Pan − *National Synchrotron Radiation Laboratory, University of Science and Technology of China, Hefei, Anhui 230029, China;* orcid.org/0000-0002-9360-3809

Zhenrong Sun − *State Key Laboratory of Precision Spectroscopy, East China Normal University, Shanghai 200062, China*

Complete contact information is available at: https://pubs.acs.org/10.1021/jacs.6c04482

Notes

The authors declare no competing financial interest.

■ ACKNOWLEDGMENTS

This work was conducted under a Memorandum of Understanding (MOU) between the East China Normal University (ECNU), the University of Hawaii at Manoa (UHM), and the National Synchrotron Radiation Laboratory (NSRL). Z.S. and T.Y. thank the support from the National Natural Science Foundation of China (Grants No. 12034008, 12250003, and 92461301). T.Y. thanks the National Natural Science Foundation of China (Grant No. 12274140), the Xinjiang Tianchi Talent Program (2023), the Program for Professor of Special Appointment (Eastern Scholar) at Shanghai Institutions of Higher Learning, the Young Top-Notch Talent Support Program of Shanghai, and the Natural Science Foundation of Shanghai (Grant No. 22ZR1421400) for funding. R.I.K. thanks the support from the U.S. National Science Foundation (NSF), Division of Astronomical Sciences (NSF AST 2403867).

■ REFERENCES

(1) Arumainayagam, C. R.; Garrod, R. T.; Boyer, M. C.; Hay, A. K.; Bao, S. T.; Campbell, J. S.; Wang, J.; Nowak, C. M.; Arumainayagam, M. R.; Hodge, P. J. Extraterrestrial prebiotic molecules: photochemistry vs. radiation chemistry of interstellar ices. *Chem. Soc. Rev.* **2019**, *48*, 2293−2314.

(2) Boogert, A. A.; Gerakines, P. A.; Whittet, D. C. Observations of the icy universe. *Annu. Rev. Astron. Astr.* **2015**, *53*, 541−581.

(3) Jørgensen, J. K.; Belloche, A.; Garrod, R. T. Astrochemistry During the Formation of Stars. *Annu. Rev. Astron. Astr.* **2020**, *58*, 727−778.
(4) Kleimeier, N. F.; Eckhardt, A. K.; Schreiner, P. R.; Kaiser, R. I. Interstellar formation of biorelevant pyruvic acid ($CH_3COCOOH$). *Chem* **2020**, *6*, 3385−3395.
(5) Glavin, D. P.; Burton, A. S.; Elsila, J. E.; Aponte, J. C.; Dworkin, J. P. The Search for Chiral Asymmetry as a Potential Biosignature in our Solar System. *Chem. Rev.* **2020**, *120*, 4660−4689.
(6) Ziurys, L. M. Prebiotic astrochemistry from astronomical observations and laboratory spectroscopy. *Annu. Rev. Phys. Chem.* **2024**, *75*, 307−327.
(7) Li, J.; Shen, Z.; Wang, J.; Chen, X.; Li, D.; Wu, Y.; Dong, J.; Zhao, R.; Gou, W.; Wang, J.; et al. Widespread presence of glycolaldehyde and ethylene glycol around sagittarius B2. *Astrophys. J.* **2017**, *849*, 115.
(8) van Gelder, M. L.; Tabone, B.; Tychoniec, Ł.; van Dishoeck, E. F.; Beuther, H.; Boogert, A. C. A.; Garatti, A. C. o.; Klaassen, P. D.; Linnartz, H.; Müller, H. S. P.; Taquet, V. Complex organic molecules in low-mass protostars on Solar System scales-I. Oxygen-bearing species. *Astron. Astrophys.* **2020**, *639*, A87.
(9) Rubin, M.; Altwegg, K.; Balsiger, H.; Berthelier, J.-J.; Combi, M. R.; De Keyser, J.; Drozdovskaya, M.; Fiethe, B.; Fuselier, S. A.; Gasc, S.; et al. Elemental and molecular abundances in comet 67P/Churyumov-Gerasimenko. *MNRAS* **2019**, *489*, 594−607.
(10) Charnley, S.; Ehrenfreund, P.; Kuan, Y.-J. Spectroscopic diagnostics of organic chemistry in the protostellar environment. *Spectrochim Acta A* **2001**, *57*, 685−704.
(11) Charnley, S.; Rodgers, S. Interstellar reservoirs of cometary matter. *Space Sci. Rev.* **2008**, *138*, 59−73.
(12) Watanabe, N.; Kouchi, A. Efficient formation of formaldehyde and methanol by the addition of hydrogen atoms to CO in H_2O-CO ice at 10 K. *Astrophys. J.* **2002**, *571*, L173.
(13) Fedoseev, G.; Cuppen, H. M.; Ioppolo, S.; Lamberts, T.; Linnartz, H. Experimental evidence for glycolaldehyde and ethylene glycol formation by surface hydrogenation of CO molecules under dense molecular cloud conditions. *MNRAS* **2015**, *448*, 1288−1297.
(14) Butscher, T.; Duvernay, F.; Theule, P.; Danger, G.; Carissan, Y.; Hagebaum-Reignier, D.; Chiavassa, T. Formation mechanism of glycolaldehyde and ethylene glycol in astrophysical ices from HCO· and ·CH_2OH recombination: an experimental study. *MNRAS* **2015**, *453*, 1587−1596.
(15) Chuang, K.-J.; Fedoseev, G.; Ioppolo, S.; Van Dishoeck, E.; Linnartz, H. H-atom addition and abstraction reactions in mixed CO, H_2CO and CH_3OH ices−an extended view on complex organic molecule formation. *MNRAS* **2016**, *455*, 1702−1712.
(16) Butscher, T.; Duvernay, F.; Rimola, A.; Segado-Centellas, M.; Chiavassa, T. Radical recombination in interstellar ices, a not so simple mechanism. *Phys. Chem. Chem. Phys.* **2017**, *19*, 2857−2866.
(17) Butscher, T.; Duvernay, F.; Danger, G.; Torro, R.; Lucas, G.; Carissan, Y.; Hagebaum-Reignier, D.; Chiavassa, T. Radical-assisted polymerization in interstellar ice analogues: Formyl radical and polyoxymethylene. *MNRAS* **2019**, *486*, 1953−1963.
(18) Layssac, Y.; Gutiérrez-Quintanilla, A.; Chiavassa, T.; Duvernay, F. Detection of glyceraldehyde and glycerol in VUV processed interstellar ice analogues containing formaldehyde: a general formation route for sugars and polyols. *MNRAS* **2020**, *496*, 5292−5307.
(19) Öberg, K. I.; Garrod, R. T.; van Dishoeck, E. F.; Linnartz, H. Formation rates of complex organics in UV irradiated CH_3OH-rich ices-I. Experiments. *Astron. Astrophys.* **2009**, *504*, 891−913.
(20) Maity, S.; Kaiser, R. I.; Jones, B. M. Formation of complex organic molecules in methanol and methanol−carbon monoxide ices exposed to ionizing radiation−a combined FTIR and reflectron time-of-flight mass spectrometry study. *Phys. Chem. Chem. Phys.* **2015**, *17*, 3081−3114.
(21) Abou Mrad, N.; Duvernay, F.; Chiavassa, T.; Danger, G. Methanol ice VUV photoprocessing: GC-MS analysis of volatile organic compounds. *MNRAS* **2016**, *458*, 1234−1241.
(22) Paardekooper, D.; Bossa, J.-B.; Linnartz, H. Laser desorption time-of-flight mass spectrometry of vacuum UV photo-processed methanol ice. *Astron. Astrophys.* **2016**, *592*, A67.
(23) Chuang, K.-J.; Fedoseev, G.; Qasim, D.; Ioppolo, S.; Van Dishoeck, E.; Linnartz, H. Production of complex organic molecules: H-atom addition versus UV irradiation. *MNRAS* **2017**, *467*, 2552−2565.
(24) de Marcellus, P.; Meinert, C.; Myrgorodska, I.; Nahon, L.; Buhse, T.; d'Hendecourt, L. L. S.; Meierhenrich, U. J. Aldehydes and sugars from evolved precometary ice analogs: Importance of ices in astrochemical and prebiotic evolution. *Proc. Natl. Acad. Sci. U. S. A.* **2015**, *112*, 965−970.
(25) Kaiser, R. I.; Maity, S.; Jones, B. M. Synthesis of prebiotic glycerol in interstellar ices. *Angew. Chem. Int. Ed.* **2015**, *54*, 195−200.
(26) Cooper, G.; Kimmich, N.; Belisle, W.; Sarinana, J.; Brabham, K.; Garrel, L. Carbonaceous meteorites as a source of sugar-related organic compounds for the early Earth. *Nature* **2001**, *414*, 879−883.
(27) Cooper, G.; Rios, A. C. Enantiomer excesses of rare and common sugar derivatives in carbonaceous meteorites. *Proc. Natl. Acad. Sci. U. S. A.* **2016**, *113*, E3322−E3331.
(28) Nuevo, M.; Cooper, G.; Sandford, S. A. Deoxyribose and deoxysugar derivatives from photoprocessed astrophysical ice analogues and comparison to meteorites. *Nat. Commun.* **2018**, *9*, 5276.
(29) Agarwal, V.; Schutte, W.; Greenberg, J.; Ferris, J.; Briggs, R.; Connor, S.; Van de Bult, C.; Baas, F. Photochemical reactions in interstellar grains photolysis of CO, NH_3, and H_2O. *Orig. Life Evol. Bios.* **1985**, *16*, 21−40.
(30) Briggs, R.; Ertem, G.; Ferris, J.; Greenberg, J.; McCain, P.; Mendoza-Gomez, C.; Schutte, W. Comet Halley as an aggregate of interstellar dust and further evidence for the photochemical formation of organics in the interstellar medium. *Orig. Life Evol. Bios.* **1992**, *22*, 287−307.
(31) Horneck, G.; Rettberg, P. *Complete Course in Astrobiology*; John Wiley & Sons, 2007.
(32) Nuevo, M.; Bredehöft, J. H.; Meierhenrich, U. J.; d'Hendecourt, L.; Thiemann, W. H.-P. Urea, glycolic acid, and glycerol in an organic residue produced by ultraviolet irradiation of interstellar/precometary ice analogs. *Astrobiology* **2010**, *10*, 245−256.
(33) Meinert, C.; Myrgorodska, I.; De Marcellus, P.; Buhse, T.; Nahon, L.; Hoffmann, S. V.; d'Hendecourt, L. L. S.; Meierhenrich, U. J. Ribose and related sugars from ultraviolet irradiation of interstellar ice analogs. *Science* **2016**, *352*, 208−212.
(34) Fedoseev, G.; Chuang, K. J.; Ioppolo, S.; Qasim, D.; Dishoeck, E. F. v.; Linnartz, H. Formation of Glycerol through Hydrogenation of CO Ice under Prestellar Core Conditions. *Astrophys. J.* **2017**, *842*, 52.
(35) Zhu, C.; Turner, A. M.; Meinert, C.; Kaiser, R. I. On the production of polyols and hydroxycarboxylic acids in interstellar analogous ices of methanol. *Astrophys. J.* **2020**, *889*, 134.
(36) Abplanalp, M. J.; Gozem, S.; Krylov, A. I.; Shingledecker, C. N.; Herbst, E.; Kaiser, R. I. A study of interstellar aldehydes and enols as tracers of a cosmic ray-driven nonequilibrium synthesis of complex organic molecules. *Proc. Natl. Acad. Sci. U. S. A.* **2016**, *113*, 7727−7732.
(37) Zhu, C.; Wang, H.; Medvedkov, I.; Marks, J.; Xu, M.; Yang, J.; Yang, T.; Pan, Y.; Kaiser, R. I. Exploitation of synchrotron radiation photoionization mass spectrometry in the analysis of complex organics in interstellar model ices. *J. Phys. Chem. Lett.* **2022**, *13*, 6875−6882.
(38) Marks, J. H.; Bai, X.; Nikolayev, A. A.; Gong, Q. a.; Zhu, C.; Kleimeier, N. F.; Turner, A. M.; Singh, S. K.; Wang, J.; Yang, J.; et al. Methanetriol−Formation of an Impossible Molecule. *J. Am. Chem. Soc.* **2024**, *146*, 12174−12184.
(39) Marks, J. H.; Bai, X.; Nikolayev, A. A.; Gong, Q. a.; McAnally, M.; Wang, J.; Pan, Y.; Fortenberry, R. C.; Mebel, A. M.; Yang, T.; et al. Methanetetrol and the final frontier in ortho acids. *Nat. Commun.* **2025**, *16*, 6468.
(40) Bai, X.; Li, C.; Luo, Y.; Gong, Q. a.; Lu, J.; Yang, J.; Pan, Y.; Sun, Z.; Eckhardt, A. K.; Sun, R.; et al. Formation of hydrogen

trioxide (HOOOH) in extraterrestrial ice analogs and its role as an oxidizer in prebiotic chemistry. *Sci. Adv.* **2025**, *11*, No. eadw5720.
(41) Gong, Q. a.; Bai, X.; Lu, J.; Yang, J.; Pan, Y.; Sun, Z.; Kaiser, R. I.; Yang, T. Formation of Polyoxymethylenes in Extraterrestrial Ice Analogs of Formaldehyde Exposed to Ionizing Radiation. *Astrophys. J.* **2025**, *994*, 70.
(42) Holland, D. M. P.; Shaw, D. A.; McSweeney, S. M.; MacDonald, M. A.; Hopkirk, A.; Hayes, M. A. A study of the absolute photoabsorption, photoionization and photodissociation cross sections and the photoionization quantum efficiency of oxygen from the ionization threshold to 490 B. *Chem. Phys.* **1993**, *173*, 315−331.
(43) Dodson, L. G.; Shen, L.; Savee, J. D.; Eddingsaas, N. C.; Welz, O.; Taatjes, C. A.; Osborn, D. L.; Sander, S. P.; Okumura, M. VUV photoionization cross sections of HO_2, H_2O_2, and H_2CO. *J. Phys. Chem. A* **2015**, *119*, 1279−1291.
(44) Batten, C.; Taylor, J. A.; Meisels, G. Photoionization processes at threshold. I. Threshold photoelectron and photoionization spectra of CO_2. *J. Chem. Phys.* **1976**, *65*, 3316−3325.
(45) May, R. A.; Smith, R. S.; Kay, B. D. The molecular volcano revisited: determination of crack propagation and distribution during the crystallization of nanoscale amorphous solid water films. *J. Phys. Chem. Lett.* **2012**, *3*, 327−331.
(46) Wang, H.; Guan, J.; Gao, J.; Li, Y.; Zhang, J.; Shan, X.; Wang, Z. Discriminating between the dissociative photoionization and thermal decomposition products of ethylene glycol by synchrotron VUV photoionization mass spectrometry and theoretical calculations. *Phys. Chem. Chem. Phys.* **2022**, *24*, 26915−26925.
(47) Taatjes, C. A.; Meloni, G.; Selby, T. M.; Trevitt, A. J.; Osborn, D. L.; Percival, C. J.; Shallcross, D. E. Direct observation of the gas-phase Criegee intermediate (CH_2OO). *J. Am. Chem. Soc.* **2008**, *130*, 11883−11885.
(48) Fujimoto, M.; Tanaka, H.; Marinho, R.; Medina, A.; Prudente, F.; Homem, M. Cross Sections and Asymmetry Parameters for Formic Acid in the Vacuum-Ultraviolet Energy Range. *J. Phys. Chem. A* **2020**, *124*, 6478−6485.
(49) Wang, J.; Turner, A. M.; Marks, J. H.; Zhang, C.; Kleimeier, N. F.; Bergantini, A.; Singh, S. K.; Fortenberry, R. C.; Kaiser, R. I. Preparation of Acetylenediol (HOCCOH) and Glyoxal (HCOCHO) in Interstellar Analog Ices of Carbon Monoxide and Water. *Astrophys. J.* **2024**, *967*, 79.
(50) Porterfield, J. P.; Baraban, J. H.; Troy, T. P.; Ahmed, M.; McCarthy, M. C.; Morgan, K. M.; Daily, J. W.; Nguyen, T. L.; Stanton, J. F.; Ellison, G. B. Pyrolysis of the Simplest Carbohydrate, Glycolaldehyde (CHO−CH_2OH), and Glyoxal in a Heated Microreactor. *J. Phys. Chem. A* **2016**, *120*, 2161−2172.
(51) Hansen, N. A.; Price, T. D.; Filardi, L. R.; Gurses, S. M.; Zhou, W. Q.; Hansen, N.; Osborn, D. L.; Zador, J.; Kronawitter, C. X. The photoionization of methoxymethanol: Fingerprinting a reactive C_2 oxygenate in a complex reactive mixture. *J. Chem. Phys.* **2024**, *160*, 124306.
(52) Bell, F.; Ruan, Q. N.; Golan, A.; Horn, P. R.; Ahmed, M.; Leone, S. R.; Head-Gordon, M. Dissociative Photoionization of Glycerol and its Dimer Occurs Predominantly via a Ternary Hydrogen-Bridged Ion−Molecule Complex. *J. Am. Chem. Soc.* **2013**, *135*, 14229−14239.
(53) Toriyama, K.; Iwasaki, M. Electron spin resonance studies on radiolysis of crystalline methanol at 4.2 K. *J. Am. Chem. Soc.* **1979**, *101*, 2516−2523.
(54) Tachikawa, H. Reaction mechanism of the radical isomerization from CH_3O to CH_2OH in frozen methanol. An ab initio MO and RRKM study. *Chem. Phys. Lett.* **1993**, *212*, 27−31.
(55) Bennett, C. J.; Kaiser, R. I. On the formation of glycolaldehyde ($HCOCH_2OH$) and methyl formate ($HCOOCH_3$) in interstellar ice analogs. *Astrophys. J.* **2007**, *661*, 899.
(56) Zhu, C.; Frigge, R.; Bergantini, A.; Fortenberry, R. C.; Kaiser, R. I. Untangling the formation of methoxymethanol (CH_3OCH_2OH) and dimethyl peroxide (CH_3OOCH_3) in star-forming regions. *Astrophys. J.* **2019**, *881*, 156.
(57) Buszek, R. J.; Sinha, A.; Francisco, J. S. The isomerization of methoxy radical: intramolecular hydrogen atom transfer mediated through acid catalysis. *J. Am. Chem. Soc.* **2011**, *133*, 2013−2015.
(58) Lee, Y.-F.; Chou, W.-T.; Johnson, B. A.; Tabor, D. P.; Sibert III, E. L.; Lee, Y.-P. Infrared absorption of CH_3O and CD_3O radicals isolated in solid para-H_2. *J. Mol. Spectrosc.* **2015**, *310*, 57−67.
(59) Green, J. C.; Decleva, P. Photoionization cross-sections: a guide to electronic structure. *Coord. Chem. Rev.* **2005**, *249*, 209−228.
(60) Leroux, K.; Krim, L. Thermal and photochemical study of CH_3OH and CH_3OH−O_2 astrophysical ices. *MNRAS* **2020**, *500*, 1188−1200.
(61) Bennett, C. J.; Hama, T.; Kim, Y. S.; KawasakI, M.; Kaiser, R. I. Laboratory studies on the formation of formic acid (HCOOH) in interstellar and cometary ices. *Astrophys. J.* **2011**, *727*, 27.
(62) Zhu, C.; Kleimeier, N. F.; Turner, A. M.; Singh, S. K.; Fortenberry, R. C.; Kaiser, R. I. Synthesis of methanediol [$CH_2(OH)_2$]: The simplest geminal diol. *Proc. Natl. Acad. Sci. U. S. A.* **2022**, *119*, No. e2111938119.
(63) Cao, Q.; Berski, S.; Latajka, Z.; Räsänen, M.; Khriachtchev, L. Reaction of atomic hydrogen with formic acid. *Phys. Chem. Chem. Phys.* **2014**, *16*, 5993−6001.
(64) Chaabouni, H.; Baouche, S.; Diana, S.; Minissale, M. Reactivity of formic acid (HCOOH) with H atoms on cold surfaces of interstellar interest. *Astron. Astrophys.* **2020**, *636*, A4.
(65) Boogert, A. C. A.; Pontoppidan, K. M.; Knez, C.; Lahuis, F.; Kessler-Silacci, J.; van Dishoeck, E. F.; Blake, G. A.; Augereau, J. C.; Bisschop, S. E.; Bottinelli, S.; et al. The c2d *Spitzer* spectroscopic survey of ices around low-mass young stellar objects.: I.: H_2O and the 5−8 μm bands. *Astrophys. J.* **2008**, *678*, 985−1004.
(66) Sallembien, Q.; Bouteiller, L.; Crassous, J.; Raynal, M. Possible chemical and physical scenarios towards biological homochirality. *Chem. Soc. Rev.* **2022**, *51*, 3436−3476.
(67) Bailey, J.; Chrysostomou, A.; Hough, J.; Gledhill, T.; McCall, A.; Clark, S.; Ménard, F.; Tamura, M. Circular polarization in star-formation regions: Implications for biomolecular homochirality. *Science* **1998**, *281*, 672−674.
(68) De Marcellus, P.; Meinert, C.; Nuevo, M.; Filippi, J.-J.; Danger, G.; Deboffle, D.; Nahon, L.; Le Sergeant d'Hendecourt, L.; Meierhenrich, U. J. Non-racemic amino acid production by ultraviolet irradiation of achiral interstellar ice analogs with circularly polarized light. *Astrophys. J., Lett.* **2011**, *727*, L27.
(69) Moore, B.; Zeng, L.; Djuricanin, P.; Cooke, I. R.; Madison, K. W.; Momose, T. Significant Chiral Asymmetry Observed in Neutral Amino Acid Ultraviolet Photolysis. *J. Am. Chem. Soc.* **2024**, *146*, 34333−34340.
(70) Garcia, A. D.; Meinert, C.; Sugahara, H.; Jones, N. C.; Hoffmann, S. V.; Meierhenrich, U. J. The astrophysical formation of asymmetric molecules and the emergence of a chiral bias. *Life* **2019**, *9*, 29.
(71) Bocková, J.; Jones, N. C.; Topin, J.; Hoffmann, S. V.; Meinert, C. Uncovering the chiral bias of meteoritic isovaline through asymmetric photochemistry. *Nat. Commun.* **2023**, *14*, 3381.
(72) Zhou, Z.; Du, X.; Yang, J.; Wang, Y.; Li, C.; Wei, S.; Du, L.; Li, Y.; Qi, F.; Wang, Q. The vacuum ultraviolet beamline/endstations at NSRL dedicated to combustion research. *J. Synchrotron Radiat.* **2016**, *23*, 1035−1045.
(73) Bouilloud, M.; Fray, N.; Bénilan, Y.; Cottin, H.; Gazeau, M. C.; Jolly, A. Bibliographic review and new measurements of the infrared band strengths of pure molecules at 25 K: H_2O, CO_2, CO, CH_4, NH_3, CH_3OH, HCOOH and H_2CO. *MNRAS* **2015**, *451*, 2145−2160.
(74) Drouin, D.; Couture, A. R.; Joly, D.; Tastet, X.; Aimez, V.; Gauvin, R. CASINO V2.42: a fast and easy-to-use modeling tool for scanning electron microscopy and microanalysis users. *Scanning* **2007**, *29*, 92−101.
(75) Gupta, S. Peak decomposition using Pearson type VII function. *Appl. Crystallogr.* **1998**, *31*, 474−476.

https://doi.org/10.1021/jacs.6c04482
J. Am. Chem. Soc. 2026, 148, 22979−22989